ELSEVIER

Thermochimica Acta 302 (1997) 87–91

thermochimica acta

Thermal properties and devitrification behaviour of $(2.5-x)CaO.x/3Y_2O_3.2SiO_2$

R. Fresa, A. Costantini*, F. Branda

Dipartimento di Ingegneria dei Materiali e della Produzione, Università di Napoli, Piazzale Tecchio, 80125 Napoli, Italy

Received 3 February 1997; received in revised form 9 May 1997; accepted 11 May 1997

Abstract

The effect on thermal properties and non-isothermal devitrification of substituting CaO by Y_2O_3, in a glass of composition 2.5 $CaO.2SiO_2$ was studied. The glass samples were submitted to thermal analysis (DTA) and X-ray diffraction analysis. The trends with the composition of the glass transformation, T_g, softening, T_s temperature and the activation energy of crystal growth, E_c, can be explained on the basis of the increase of the structural rigidity when Ca^{2+} ions are substituted by Y^{3+} ions; stronger bonds to the oxygen are, indeed, expected. In all the devitrified samples $CaO.SiO_2$ crystals form together with a secondary calcium silicate phase. The pattern of the Y_2O_3 free glass shows that the $\alpha CaO.SiO_2$ is also formed in the temperature range 900–1000°C. When $x = 1.0$ a new, crystalline phase appears, which could not be identified by means of JCPDS cards. The activation energy for crystal growth was $E_c = 640 \pm 25.1$ kJ/mole, regardless of composition. Devitrification involved a mechanism of surface nucleation: however, as the samples softened and sintered before devitrifying, surface nuclei behaved as bulk nuclei. © 1997 Elsevier Science B.V.

Keywords: Activation energies; Calcium yttrium silicate; Crystal growth; DTA; Non-isothermal devitrification; Tg

1. Introduction

It is known that glasses of the system $CaO–SiO_2$ that have a CaO molar fraction in the range 0.30–0.55 are bioactive [1,2]. The addition of yttrium oxide to silicates enables glasses to be obtained with high elastic moduli and hardness [3]. Yttrium additions have also proved to be useful in obtaining glass-ceramics which have interesting properties. Workable glass ceramics have been obtained in the system $CaO-Al_2O_3-Y_2O_3-SiO_2$ [4]. Refractory glasses have been obtained in the system $Y_2O_3-Al_2O_3-SiO_2$ [5]. Recently, it was found [6,7] that the non-isothermal devitrification of glasses of the system $CaO-La_2O_3(MgO)-SiO_2$ has peculiar characteristics. They devitrify through a surface nucleation mechanism. However, because in the temperature range of efficient crystal growth, softening and sintering occur, surface nuclei behave virtually as bulk nuclei. This was well supported by SEM observations of samples devitrified during a DSC run [8].

In this paper the thermal properties and the study of the devitrification behaviour of glasses of the system $CaO-Y_2O_3-SiO_2$ are reported. In particular, the effect of the substitution of CaO by Y_2O_3 in the glass of composition 2.5 $CaO.2SiO_2$ has been studied. The substitution was such so as not to change the O/Si molar ratio.

*Corresponding author.

PII S0040-6031(97)00210-4

2. Experimental

Glasses of composition expressed by the following general formula:

$$(2.5 - x)\mathrm{CaO}.x/3\mathrm{Y_2O_3}.2\mathrm{SiO_2}$$

where $0 \leq x \leq 1.0$ were prepared by melting analytical grade reagents, Y_2O_3, $CaCO_3$, SiO_2 in a platinum crucible in an electric oven for 4 h, in the temperature range 1400–1600°C. The melts were quenched by plunging the bottom of the crucible into cold water.

Thermal analysis was carried out by means of a Netzsch differential scanning calorimeter (DSC) model 404 M, on about 50.0 mg powdered samples, −170 + 230 mesh, at various heating rates. Powdered Al_2O_3 was used as reference material. The non-isothermal devitrification was also studied. The kinetic parameters were determined by using Eqs. (1) and (2).

$$\ln \beta = -E_c/RT_p + \text{const.} \quad (1)$$

$$\ln \Delta T = -mE_c/RT + \text{const.} \quad (2)$$

Eqs. (1) and (2) can be derived from the well-known following equation [9,10]:

$$-\ln(1 - \alpha) = (AN/\beta^m)\exp(-mE_c/RT) \quad (3)$$

where α is the crystallization degree, N is the nuclei number, A is a constant, β is the heating rate, ΔT and T_p are the deflection from the base line and the peak temperature taken as indicated in Fig. 1, T is the temperature.

As in inorganic glasses, the devitrification exothermic peak occurs in a temperature range higher than that of efficient nucleation [11], E_c is the activation energy of crystal growth. The parameter m depends upon the mechanism and morphology of crystal growth. It ranges from $m = 1$ for 3-dimensional growth [9,10]. Eqs. (1) and (2) can be derived from it by supposing: (1) α at peak temperature is not dependent on the heating rate, [12]; (2) ΔT is proportional to the instantaneous reaction rate [13,14] and (3) in the initial part of the DTA crystallization peak, the change in the temperature has a much lower effect than α on the ΔT [15].

Devitrified samples were analyzed by computer-interfaced X-ray (CuK_α) powder diffractometry (XRD) using a Philips diffractometer model PW1710, with a scan speed of $1^\circ\,\mathrm{min}^{-1}$ and a built-in computer search program. The crystalline phases were identified by means of JCPDS cards.

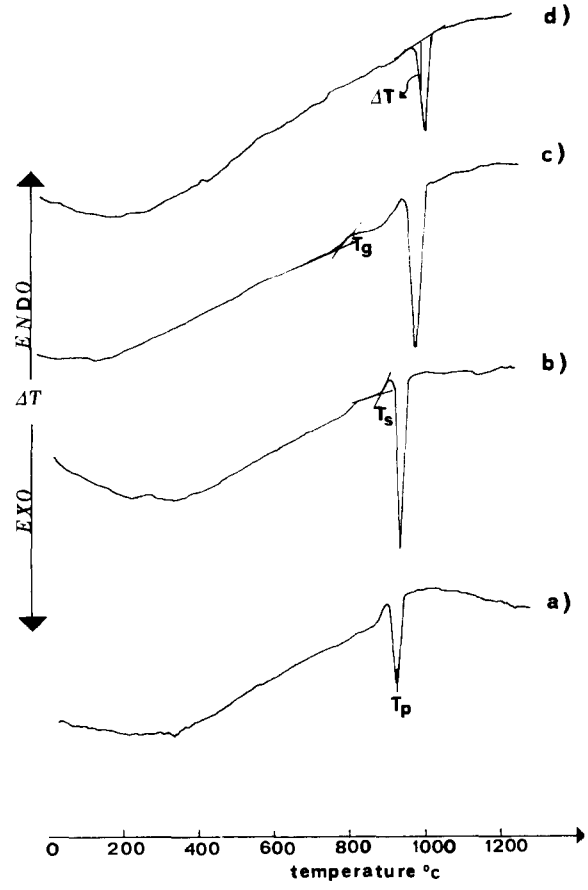

Fig. 1. DTA curves recorded at 10°C/min heating rate on fine (63–90 μm) powdered samples. (a) $x = 1.0$; (b) $x = 0.6$; (c) $x = 0.2$; (d) $x = 0$.

3. Results

Fig. 1 shows the DTA curves. After a slope change in the glass transformation range, an exothermic peak appears, in all cases, due to devitrification. All curves showed a second slope change that appeared just before the devitrification took place. It was due to softening and sintering of the sample and the consequent variation of heat transfer coefficient as the sample–sample holder contact changes. As a matter of fact, in these cases, the initially powdered samples

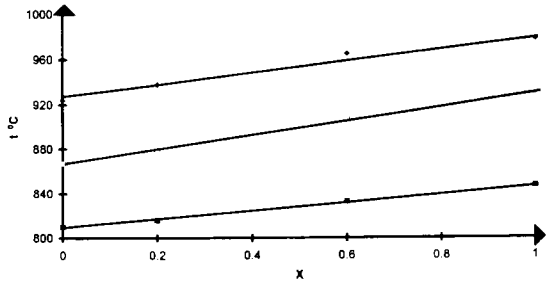

Fig. 2. Plot of the glass transformation, T_g (■), softening, T_s (□), and devitrification exo-peaks, T_p (◆), versus composition (x).

were recovered from the sample holder as more or less porous bodies. The softening effect was more pronounced in glasses for which the value of x is low.

As illustrated in Fig. 1, the glass transformation temperature, T_g, and the softening temperature, T_s, were taken as the onset temperature in the glass transformation and the softening ranges, respectively. Their values are plotted against the glass composition, expressed as the x values of the general formula, in Fig. 2. In the same figure the DTA exothermic peak temperatures, T_p, are also shown. As can be seen, all of them increased as the Y_2O_3 content was increased.

Fig. 3 shows the X-ray diffraction patterns of the samples submitted to a DTA run stopped just after the exothermic peak. The lines were attributed by means of the JCPDS cards. In all patterns, the lines of wollastonite (JCPDS card 27/88) appear. In the (a) pattern ($x = 0$) the lines of pseudo-wollastonite, $\alpha CaO.SiO_2$ (JCPDS card 19/248) and $3CaO.SiO_2$ (JCPDS card 11-593) were also present. It is interesting to observe that $\alpha CaO.SiO_2$ is the high temperature phase which, in the phase diagram $CaO–SiO_2$ is reported to be stable above 1125°C. In the patterns ((b), (c) and (d)), they are substituted by the lines of $2CaO.SiO_2$ (JCPDS card 24-234); in the (d) pattern ($x = 1.0$) some other lines appear that could not be identified by means of JCPDS cards.

In Fig. 4 the plots of $\ln \beta$ versus $1/T_p$ are reported. In Fig. 5 the plots of $\ln \Delta T$ versus $1/T$ are reported for powdered samples taken from DTA curves recorded at 10°C/min. According to Eqs. (1) and (2) straight lines were obtained. Their slopes allow the determination of values of E_c and mE_c (Fig. 6). The substitution of CaO by Y_2O_3 appears to have no effect on E_c and mE_c. Their ratio gives a value of $m \cong 2$.

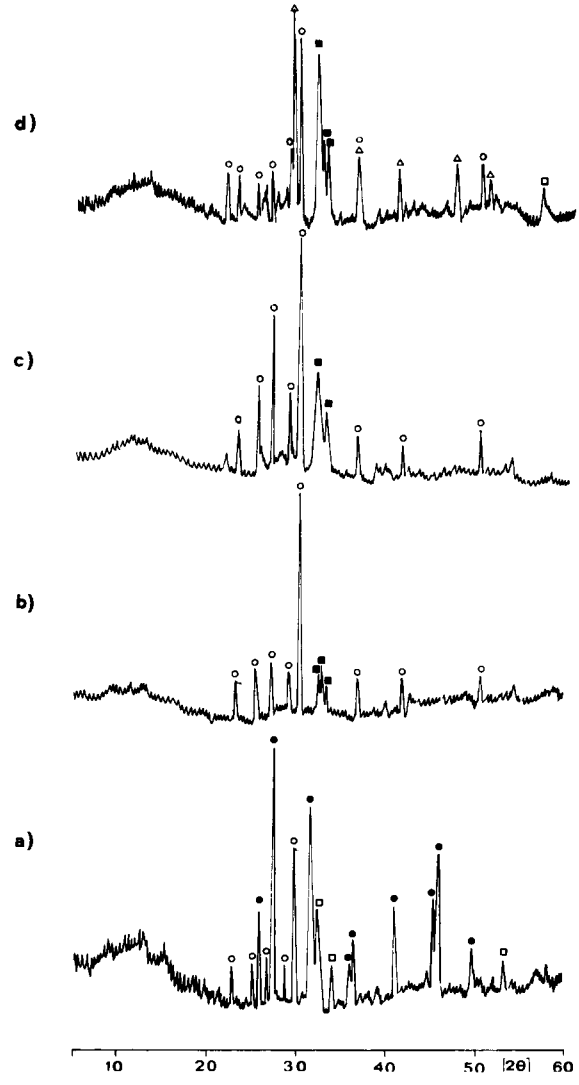

Fig. 3. X-ray diffraction patterns of samples devitrified during a DTA run: (a) $x = 0$. (b) $x = 0.2$; (c) $x = 0.6$; (d) $x = 1.0$; (○) wollastonite; (JCPDS card 27/88); (•) pseudo-wollastonite (JCPDS card 19/248); (□) $3CaOSiO_2$ (JCPDS card 11/593); (■) $2CaOSiO_2$ (JCPDS card 24/234); (△) unknown phase.

4. Discussion

The increase of T_g as the CaO is substituted by Y_2O_3 can be explained by taking into account the fact that the glass transformation temperature depends on the density of covalent cross-linking and the number and strength of the cross-links between the cation and

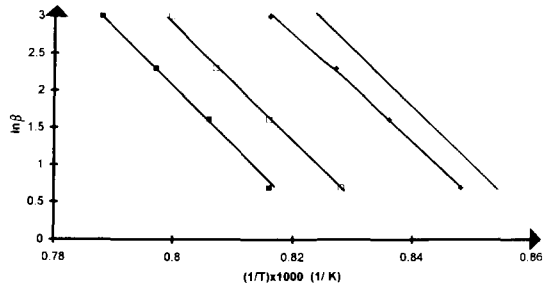

Fig. 4. Plot of ln β versus $1/T_p$. $x = 0$ (◇); $x = 0.2$; (◆) $x = 0.6$ (□); $x = 1.0$ (■).

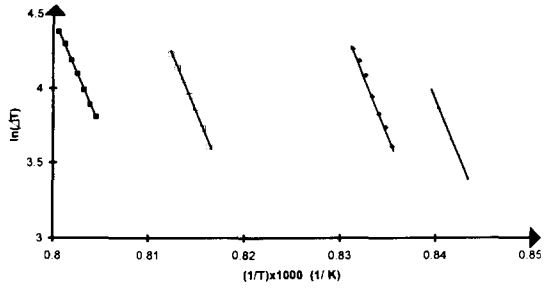

Fig. 5. Plot of ln ΔT versus $1/T$. $x = 0$ (◇); $x = 0.2$ (◆); $x = 0.6$ (□); $x = 1.0$ (■).

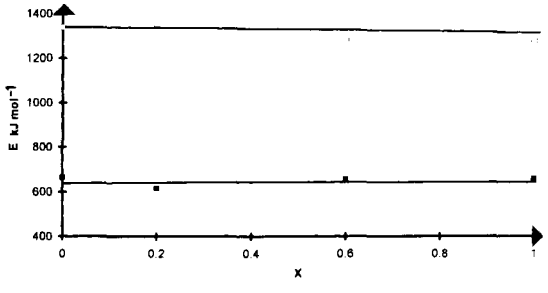

Fig. 6. Plot of the activation energy for crystalline growth, E_c (■) and mE_c (□) versus composition (x).

oxygen atoms [16]. It is worth remembering that CaO and Y_2O_3 are reported to be modifier oxides [17]. Therefore, in the studied series, the density of covalent cross-linking does not change because the molar ratio O/Si is constant. When this happens, it was found that [18,19] the changes of T_g, when a modifier oxide is substituted for another one, can be related to the coordination number and field strength Z/r^2 of the modifier cation, where Z is the charge and r the radius. Ca^{2+} and Y^{3+} have the same coordination number in their pure oxide structure [17] otherwise Y^{3+} has a greater field strength (3.76 A^{-2} instead of 2.04 A^{-2}) and a greater single bond strength in the pure oxide structure (210 kJ/mol instead of 130 kJ/mol) than Ca^{2+} has. The T_g increase can therefore be ascribed to the greater strength of the cross-links between the Y^{3+} cation and oxygen atoms. A similar explanation can be made for the increasing trend of the T_s curves.

The evolution of the XRD patterns shown in Fig. 3 is easily explained. In fact the formation of a secondary phase poorer in calcium, when CaO is substituted with Y_2O_3, ($2CaOSiO_2$ instead of $3CaOSiO_2$), can be attributed to the progressive reduction of the calcium amount. In the devitrified Y_2O_3 richer glass, the unknown phase, which is the majority one, could be supposed to have Y_2O_3 and SiO_2 as basic components.

Regarding the activation energies of crystal growth it is worth remembering that E_c is usually equal to the viscous flow activation energy E_η [11]. E_η should increase as CaO is substituted by Y_2O_3, as long as this involves the structure rigidity being increased, as discussed earlier. Otherwise, the viscosity depends on the temperature according to the Vogel–Fulker–Tamman equation [20] which implies that E_η continuously decreases as the temperature increases. Taking into account the increasing trend of T_p shown in Fig. 2, the constancy of the values shown in Fig. 6 suggests that the two effects compensate each other.

Usually in the case of finely powdered samples, owing to their high specific surface, a value $m = 1$ is expected [15]. Instead, in the case of the studied glasses, a value $m = 2$ was found. Similar values were found in the case of the glasses whose composition can be expressed as:

$$(2 - x)CaO.x/3La_2O_3.2SiO_2$$

$$(2 - x)CaO.xMgO.2SiO_2$$

In these cases the anomalously high values of m for the finely powdered samples were explained by admitting that, as a result of softening and sintering occurring just before devitrification, the surface nuclei formed in the glass transformation range behave as bulk nuclei [6,7]. This hypothesis was well supported by SEM and optical microscopy [8,21] observations.

The DSC curves of the studied glasses, reported in Fig. 1, show that they soften just before devitrifying;

therefore the same hypothesis can be put forward for the studied glasses reported in this paper.

5. Conclusions

The glass transformation, T_g, and softening, T_s, temperatures plots suggest that the substitution of Y_2O_3 to CaO caused the structure rigidity to increase.

In all devitrified samples, the lines of wollastonite (JCPDS card 27-88) and of a secondary calcium silicate phase appear. The XRD pattern of the free Y_2O_3 sample also shows the lines of pseudo-wollastonite (JCPDS card 19/248) which in the CaO–SiO_2 phase diagram is reported to be stable only above 1125°C. It is relevant that, on the contrary, the devitrified product was obtained in the temperature range 900–1000°C. In the $x = 1.0$ devitrified samples, another crystalline phase is formed whose reflections were not identified by means of JCPDS cards. Y_2O_3 and SiO_2 were considered to be the basic components.

The activation energy for crystal growth E_c was 640 ± 25.1 kJ/mole regardless of composition. Devitrification involves a mechanism of surface nucleation, but, owing to softening and sintering, surface nuclei behave as bulk nuclei.

References

[1] L.L. Hench, Bioceramics: From concept to clinic, J. Am. Cer. Soc., 74(7) (1991) 1487–1510.

[2] T. Kokubo, Novel bioactive materials derived from glasses, Proc. XVII International Congress on Glass, Madrid, Vol. 1, Bol. Soc. Esp. Ceram. Vid., 31-C1 (1992) 119–137.

[3] A. Makishima, Y. Tamura and T. Sakaino, Elastic moduli and refractive indices of aluminosilicate glasses containing Y_2O_3, La_2O_3 and TiO_2, J. Am. Cer. Soc., 61(5-6) (1978) 247.

[4] A. Makishima, M. Asami and Y. Ogura, A machinable calcia-alumina-yttria-silica glass-ceramic, J. Am. Cer. Soc., 72(6) (1989) 1024.

[5] I. Arita, D. Wilkinson and G. Purdy, Crystallization of yttria-alumina-silica glasses, J. Am. Cer. Soc., 75(12) (1992) 3315.

[6] A. Costantini, R. Fresa, A. Buri and F. Branda, Thermal properties and devitrification behaviour of $(2-x)$CaO.x/$3La_2O_3.2SiO_2$ glasses, Silicates Industriels, 7–8 (1996) 171–175.

[7] A. Costantini, F. Branda and A. Buri, Thermal properties and devitrification behaviour of $(1+x)$CaO.$(1-x)$MgO.$2SiO_2$ glasses, J. Mat. Science, 30 (1995) 1561–1564.

[8] F. Branda, A. Costantini, A. Buri and A. Tomasi, Devitrification behaviour of CaO-MgO(Y_2O_3)-SiO_2 glasses, J. Therm. Analysis, 41 (1994) 1479–1487.

[9] K. Matusita and S. Sakka, Kinetic study of non-isothermal crystallization of glass by thermal analysis, Bull. Inst. Chem. Res. Kyoto Univ., 59 (1981) 159–171.

[10] D.R. MacFarlane, M. Matecki and M. Poulain, Crystallization in fluoride glasses devitrification on reheating, J. Non.-Cryst. Solids, 64 (1984) 351–362.

[11] K. Matusita and S. Sakka, Kinetic on crystallization of glass by differential thermal analysis-criterion on application of Kissinger plot, J. Non-cryst. Solids, 38–39 (1980) 741–6.

[12] P.G. Boswell, On the calculation of activation energies using a modified Kissinger method, J. Am. Cer. Soc., 75(12) (1992) 3315.

[13] H.J. Borchardt and F. Daniels, The application of differential thermal analysis to the study of reaction kinetics, J. Am. Chem. Soc., 79 (1957) 41–46.

[14] K. Akita and M. Kase, Relationship between the DTA peak and the maximum reaction rate, J. Phys. Chem., 72 (1968) 906–913.

[15] A. Marotta, A. Buri and F. Branda, Surface and bulk crystallization in non-isothermal devitrification of glasses, Thermochim. Acta, 40 (1980) 397–404.

[16] N.H. Ray, Composition–property relationships in inorganic oxide glasses, J. Non-Cryst. Solids, 15 (1974) 423–434.

[17] H. Rawson, Inorganic Glass Forming Systems, Academic Press, London and New York, 1967 pp. 24-5.

[18] A. Buri, D. Caferra, F. Branda and M. Marotta, Relationship between composition and glass transition temperature in Na_2O-M_2O_3-SiO_2 glasses (M = Ga, In, Sc, Y, La), Phys. Chem. Glasses, 23(1) (1982) 37–40.

[19] F. Branda, A. Buri, D. Caferra and A. Marotta, The effect of mixing of network-modifiers on the transformation temperature of silicate glasses, J. Non-Cryst. Solids, 54 (1983) 193–198.

[20] H. Scholze (Ed.), Le Verre, Institut du verre, Paris, 1980, p. 69.

[21] F. Branda, A. Costantini and A. Buri, Non-isothermal devitrification behaviour of diopside glass, Thermochim. Acta, 217 (1993) 207–212.